Fine-structure population distributions of $O(^3P_j)$ in the $H+O_2$ reaction and the photolysis of NO_2

H.-G. Rubahn [1], W.J. van der Zande [2], R. Zhang [3], M.J. Bronikowski and R.N. Zare
Department of Chemistry, Stanford University, Stanford, CA 94305-5080, USA

Received 16 August 1991

The relative populations of the oxygen-atom fine-structure levels ^3P_j have been measured for the bimolecular reaction $H+O_2 \rightarrow OH+O$ and the unimolecular reaction $NO_2+h\nu \rightarrow NO+O$ using two-photon laser-induced fluorescence. In this method the $3s\,^3S_{j''} \leftarrow 3p\,^3P_{j'}$ fluorescence intensity at 845 nm is recorded following the two-photon transition $3p\,^3P_{j'} \leftarrow 2p\,^3P_j$ at 226 nm. In the $H+O_2$ reaction, the fine-structure distribution is approximately in the ratio of the statistical degeneracies (5:3:1) at a collision energy of 1.6 eV, whereas at a collision energy of 2.4 eV the population favors the fine-structure levels with lower energies. For NO_2 photolysis, the $O(^3P_j)$ distribution is described by a temperature of 200 K at 355 nm, whereas at 226 nm the $O(^3P_j)$ distribution is inverted, i.e. the population distribution favors fine-structure levels with higher energies. Those observations are compared with predictions from a model in which the kinetic energy of the recoiling products is responsible for fine-structure changing transitions.

1. Introduction

In most bimolecular reactions (full collisions) and photodissociation processes (half collisions), the resulting products have an open-shell electronic structure characterized by fine-structure splittings that result from magnetic interactions (spin–orbit coupling). Despite the prevalence of open-shell products, little attention is given to fine-structure population distributions because such distributions are often difficult to quantify and because the theoretical interpretation of these branching ratios is at a primitive stage of development [1]. The advent of laser techniques for product state analysis has made it possible to determine fine-structure population distributions for those systems whose spectroscopy is well understood. Such measurements may spur theorists to consider more deeply how these fine-structure distributions mirror the dynamics of a bimolecular or unimolecular reaction.

In this paper we concentrate on elementary processes in which a ground-state oxygen atom is a product. Specifically, we study the $O(^3P_j)$ fine-structure population distribution for the bimolecular reaction $H+O_2 \rightarrow OH+O$ and the unimolecular dissociation process $NO_2+h\nu \rightarrow NO+O$. For the oxygen atom, $^3P_2$ is the lowest-lying multiplet, $^3P_1$ lies 158.5 cm^{-1} above $^3P_2$, and $^3P_0$ lies 68 cm^{-1} above $^3P_1$ [2]. Tunable UV and VUV lasers make the interrogation of the $O(^3P_j)$ fine-structure levels possible. Miyawaki et al. [3] have used one-photon laser-induced fluorescence (LIF) at 130 nm ($3s\,^3S \leftarrow 2p\,^3P$). Bamford, Jusinksi and Bischel [4] have used two-photon LIF at 226 nm ($3p\,^3P_{j'} \leftarrow 2p\,^3P_j$) in which either the $3s\,^3S_{j''} \leftarrow 3p\,^3P_{j'}$ or $2p\,^3P_{j''} \leftarrow 3p\,^3P_{j'}$ transition was monitored, and several groups [4–6] have developed (2+1) resonance-enhanced multiphoton ionization (REMPI) via the $3p\,^3P_{j'}$ level. By now, the photolytically generated $O(^3P_j)$ distribution has been analyzed for a number of molecules, including NO_2 [3,7], SO_2 [8], O_3 [9], O_2 [5,10], CO_2 [7] and CO [11]. In addition, the $O(^3P_j)$ atoms produced in the reaction $H+O_2$ at 2.1 and 2.5 eV collision

[1] Permanent address: MPI für Strömungsforschung, Bunsenstrasse 10, W-3400 Göttingen, Germany.
[2] Permanent address: FOM-Institute for Atomic and Molecular Physics, Kruislaan 407, 1098 SJ Amsterdam, The Netherlands.
[3] Present address: IBM Almaden Research Laboratory, Department K92, 650 Harry Road, San Jose, CA 95120, USA.

energies have been reported by Matsumi et al. [6]. We describe here our measurements of the $O(^3P_j)$ fine-structure population distribution via two-photon LIF in which the red fluorescence (845 nm) is monitored. We apply this method to examine the $O(^3P_j)$ fine-structure distribution in the $H+O_2$ reaction at collision energies of 1.6 and 2.4 eV and in the photolysis of NO_2 at 355 nm (0.52 eV excess energy), 266, and 226 nm (2.4 eV) when NO_2 is at room temperature or cooled by nozzle beam expansion. A comparison of our relative population distribution will be made with those obtained by other workers under nearly comparable conditions.

2. Experimental

The experimental setup has been described in detail elsewhere [12,13]. As shown in fig. 1, two counterpropagating laser beams are focused and overlapped in the center of a reaction vessel in which reactant gases are mixed with a total pressure on the order of 100 mTorr (10 Pa). The photolysis laser beam is focused by a 1 m focal length lens to a spot size of approximately 1 mm in diameter. The probe laser is focused by a 0.5 m focal length lens to a spot size of approximately 0.2 mm in diameter. Laser-induced fluorescence is collected perpendicular to the laser beams and detected with a red-sensitive photomultiplier (RCA 31034A) using a gated detector with a 50 ns window. The delay between the photolysis laser and the probe laser is 30 ns; the gated detector is opened immediately after the probe laser is fired. Under these conditions, collisional relaxation of the $O(^3P_j)$ product is negligible.

Analysis of the fine-structure population distributions of the $O(^3P_j)$ atom relies upon fluorescence resulting from the $3p\,^3P_{j'} \leftarrow 2p\,^3P_j$ two-photon transitions near 226 nm. This wavelength is generated by mixing 1064 nm light (the Nd:YAG fundamental) with the doubled output of a Nd:YAG-pumped dye laser (Quantel TDL50; rhodamine 550 dye). The probe laser has a pulse energy of 1.5 mJ and a bandwidth of 0.2 cm^{-1}. Fluorescence was detected at 845 nm from the $3s\,^3S_{j''} \leftarrow 3p\,^3P_{j'}$ transition (lifetime 35 ns [4]). The $3p\,^3P_{j'}$ fine-structure levels are split by 0.7 and 0.2 cm^{-1}. This splitting was not resolved. By integrating the fluorescence intensity, the signal is directly proportional to the relative population of the $O(2p\,^3P_j)$ fine-structure levels, as shown by Saxon and Eichler [14]. With the use of partially crossed polarizers, the probe laser power was kept low (<100 μJ/pulse) to minimize probe-laser-induced photolysis as well as amplified spontaneous emission (ASE). Huang and Gordon [7,10] have shown that ASE can be a source of experimental error.

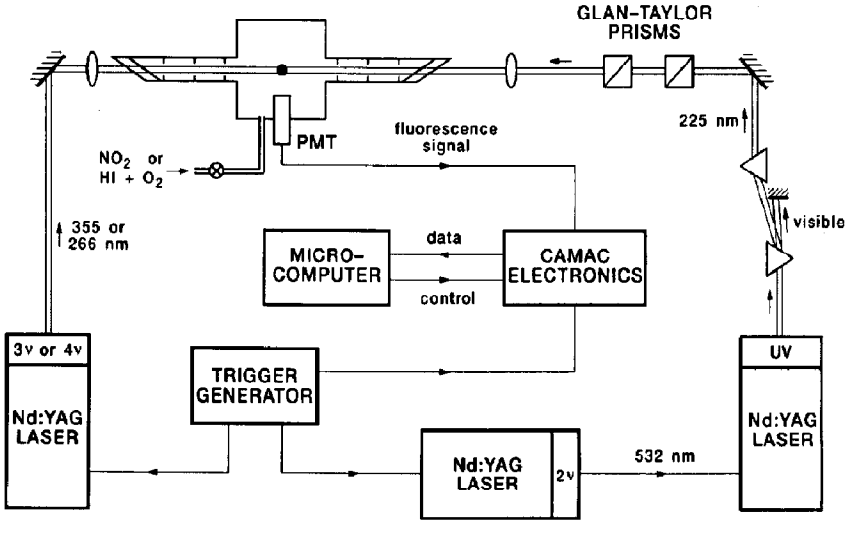

Fig. 1. Schematic of the experimental setup.

For the study of NO_2 photolysis, 355 and 266 nm laser pulses were directed into the reaction vessel. These wavelengths are generated directly as the third and fourth harmonics of the 1064 nm output from a Nd:YAG laser (Quanta Ray DCR 2A). In addition, probe-laser-induced photolysis of NO_2 can be studied at a wavelength of 226 nm.

A microwave discharge source was used to generate room-temperature oxygen atoms from pure O_2. This allowed a test of the reliability of the detection method. The relative population of the $O(^3P_j)$ multiplet levels was described by a temperature of 293 ± 13 K, giving us confidence in our detection method.

In the study of NO_2 photodissociation, NO_2 could be introduced into the vessel via a pulsed nozzle (General Valve, Inc., diameter of orifice 500 μm, measured pulse duration 600 μs) to study the effect of rotational cooling of reagents on the product oxygen-atom fine-structure distribution. In this study, only the probe-laser-induced photolysis was investigated.

The $H+O_2$ reaction was initiated by photolysis of HI at 266 or at 226 nm (the probe-laser wavelength). The collision energies of the resulting H atoms at 266 nm are 1.6 and 0.7 eV, resulting from production of I atoms in its ground fine-structure level ($^2P_{3/2}$) or excited fine-structure level ($^2P_{1/2}$). At 226 nm, the collision energies of the H atoms are 2.4 and 1.5 eV. The experimental technique developed by Rinnen et al. [15] has been used to remove the contribution of reaction products formed after photolysis of the HI by the focused probe laser. For this purpose the time delay between the photolysis and probe lasers was varied shot by shot between $\tau = 15$ ns and $\tau = 70$ ns. The difference in the measured fluorescence signal as a function of time delay then reflects the buildup of product oxygen atoms induced by the 266 nm photolysis laser itself. The probe-laser-induced reaction contributes equally to both signals, and this contribution is eliminated by subtraction. The fluorescence signals, accumulated over 10–40 laser shots, were corrected for long-term laser power fluctuations before being converted to fine-structure relative populations. The number of shots accumulated per point was varied depending on the signal intensity to obtain a satisfactory signal-to-noise ratio.

3. Results and discussion

3.1. NO_2 photolysis

Fig. 2 shows the LIF spectra of the $O(^3P_j)$ product of the photodissociation process $NO_2 + h\nu \rightarrow NO + O$ at three different photolysis wavelengths. Table 1 summarizes the relative population distributions and compares these results to those obtained from a microwave discharge of O_2, which gives a statistical distribution at a temperature of 293 ± 13 K, and with a theoretical distribution for infinite temperature. It is seen that the population in the higher fine-structure levels grows with increasing photolysis energy.

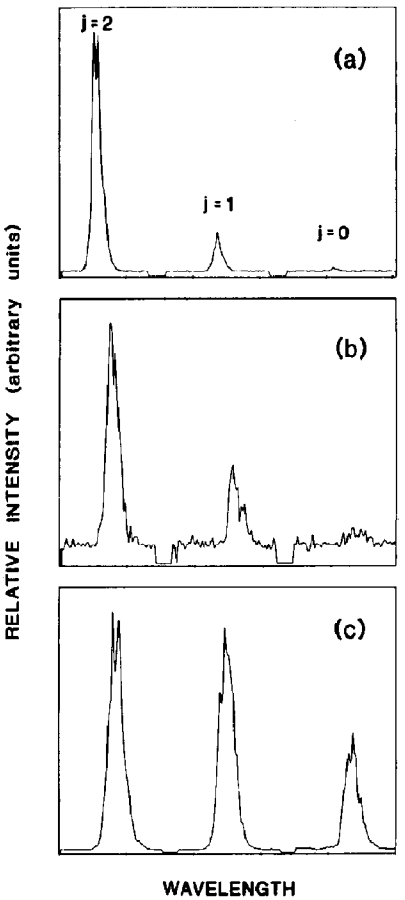

Fig. 2. LIF spectra of $O(^3P_j)$ lines measured using detection of the 845 nm fluorescence from the two-photon excitation near 226 nm. Photolysis of NO_2 is induced at (a) 355 nm, (b) 266 nm, and (c) ≈226 nm.

Table 1
Measured $O(^3P_j)$ distributions from photolysis of NO_2. The errors in parentheses represent one standard deviation

Conditions	$j=2$	$j=1$	$j=0$	Ref.
microwave discharge [a]	1	0.27(1)	0.07(1)	this work
statistical [b]	1	0.60	0.20	
355 nm photolysis, bulk	1	0.18(1)	0.04(1)	this work
355 nm photolysis, seeded beam (1) [c]	1	0.19(4)	0.03(1)	[3]
351 nm photolysis, bulk	1	0.15(3)	0.07(3)	[7]
337 nm photolysis, seeded beam (1) [c]	1	0.23(5)	0.04(1)	[3]
266 nm photolysis, bulk	1	0.23(2)	0.07(2)	this work
266 nm photolysis, seeded beam (1) [c]	1	0.17(4)	0.03(1)	[3]
226 nm photolysis, bulk	1	0.71(3)	0.25(3)	this work
226 nm photolysis, neat expansion (1) [d]	1	0.68(3)	0.27(1)	this work
226 nm photolysis, neat expansion (2) [d]	1	0.61(3)	0.22(1)	this work
226 nm photolysis, neat expansion (3) [d]	1	0.52(4)	0.20(1)	this work
226 nm photolysis, seeded beam (1) [c]	1	0.50(5)	0.17(3)	this work
226 nm photolysis, seeded beam (2) [c]	1	0.50(5)	0.17(3)	this work
226 nm photolysis, bulk	1	0.59(9)	0.26(4)	[7]
226 nm photolysis, bulk	1	0.62(6)	0.29(8)	[18]
212 nm photolysis, seeded beam (1) [c]	1	0.35(7)	0.08(1)	[3]

[a] This distribution reflects a temperature $T=293(13)$ K.
[b] Reflecting the $2j+1$ degeneracy factors (i.e. infinite temperature).
[c] (1) 10:1 He:NO_2, (2) 100:1 Ne:NO_2 560 Torr stagnation pressure.
[d] (1) 72 Torr, (2) 230 Torr, (3) 590 Torr stagnation pressure.

At a photolysis wavelength of 355 nm, the $O(^3P_j)$ fine-structure distribution is described by a temperature of approximately 200 K; at 266 nm, this distribution only changes moderately; whereas at 226 nm, the distribution has a negative temperature, i.e. higher multiplet levels are more populated than lower ones, after correcting for the $(2j+1)$ statistical degeneracy of each level j. We note that at 226 nm, there is sufficient energy to form $NO+O(^1D)$. Clearly, some drastic change occurs on decreasing the photolysis wavelength.

In a separate experiment the dependence of the observed LIF signal on probe laser power was investigated. For 355 nm photolysis, the LIF signal varies as the square of the probe laser power, which is expected for a two-photon process. In contrast, for 226 nm photolysis, the LIF signal varies as the cube of the probe laser power, as anticipated for a process in which the same wavelength causes (one-photon) photolysis as well as two-photon LIF. The detection sensitivity for $O(^3P_j)$ is approximately 4×10^9 atoms cm^{-3}, which appears to be an order of magnitude more sensitive than the (2+1) REMPI detection scheme reported by Sultan, Baravian and Jolly [16].

We observe changes in the measured distributions when NO_2 is expanded from a pulsed nozzle. As seen in table 1, the distribution becomes colder with increasing stagnation pressure. This effect is independent of whether the stagnation pressure stems from NO_2 itself or a seeding gas, indicating that it is not a consequence of the formation of NO_2 dimers or clusters in the expansion. Also, because NO_2 is photolyzed and $O(^3P)$ is probed within the same laser pulse (i.e. within a maximum time delay of 5 ns of each other), the O atoms experience negligible cooling of the translational and internal degrees of freedom within the nozzle beam before they are detected. Such cooling has been seen to pool population in the lowest fine-structure state in NH, for example [17]. Thus, although the available energy upon rotational cooling is very small (2%) with respect to the observed changes, it appears that the rovibrational state of the NO_2 influences directly the photodissociation dynamics, with lower energy NO_2 states giving rise to electronically "colder" O atoms.

A variety of techniques has been used to probe the fine-structure distribution of oxygen atoms produced in the photolysis of NO_2. Gordon [7] has used two-photon LIF, detecting both the 845 nm fluorescence and VUV fluorescence at 130 nm, while

Orlando et al. [18] have probed O atoms using a REMPI scheme. Both of these studies agree with the present results to within respective error bars, as seen in table 1. Miyawaki et al. [3] have determined the $O(^3P_j)$ fine-structure distribution from the photolysis of NO_2 at 355, 337, 266 and 212 nm using single-photon LIF detection. The NO_2 gas was seeded in He gas in these studies. Nevertheless, the fine-structure distributions are comparable with our results for NO_2 gas at room temperature at those wavelengths where they can be compared (see table 1). We conclude that several reliable techniques exist to determine the relative population of the $O(^3P_j)$ fine-structure levels.

Zacharias et al. [19] measured the product state distributions of the $NO(^2\Pi_\Omega, v, N)$ resulting from NO_2 photodissociation. They observed an increase in the $^2\Pi_{3/2}$:$^2\Pi_{1/2}$ ratio ($^2\Pi_{3/2}$ being the higher energy spin–orbit component) when the photolysis wavelength is changed from 351 to 307 nm. This result is in agreement with our finding that higher energy fine-structure components of $O(^3P_j)$ are increasingly populated as the photolysis wavelength is lowered.

NO_2 photolysis remains poorly understood because the dissociation process creates two open-shell fragments, allowing a variety of electronic transitions to occur as the fragments separate. Much more remains to be learned by continued experimental efforts, such as the measurement of O atom product velocity distributions as a function of photolysis wavelength.

3.2. $H+O_2 \rightarrow OH+O$ reaction

The $H+O_2 \rightarrow OH+O$ reaction has been studied previously by many workers. Emphasis has been placed on the reaction rate as a function of temperature, as determined by various kinetics studies [20–24], the internal state distributions, and on the OH reaction product as a function of initial relative collision energy, as revealed by laser-induced fluorescence [12,25–28]. In addition, various theoretical studies have been undertaken to provide insight into the reaction dynamics [1,29–31]. We concentrate our attention here on the fine-structure distribution of the $O(^3P_j)$ product.

In our studies fast H atoms are generated by photodissociation of HI at 266 and 226 nm. Because of the branching into different spin–orbit levels of the iodine atom, each photolysis wavelength produces H atoms with two different initial relative kinetic energies. At 266 nm, 64% of the H atoms have a collision energy of 1.6 eV and 36% have a collision energy of 0.7 eV. Because the $H+O_2$ reaction is endoergic with a threshold of 0.72 eV [32], the contribution of the slow H atoms can be neglected at this wavelength. At 226 nm, 90% of the H atoms have a relative collision energy of 2.4 eV and 10% have a relative collision energy of 1.5 eV, so that both photodissociation channels lead to reaction. At this wavelength, the $O(^3P_j)$ product has approximately a cubed dependence on the laser power, as would be expected.

Table 2 lists the $O(^3P_j)$ fine-structure population distributions at the two different photolysis wavelengths used. By taking into account the $I(^2P_{1/2})/I(^2P_{3/2})$ branching ratio and the increased collision rate of 2.4 eV H atoms compared to 1.5 eV H atoms, the fine-structure distribution for a collision energy of 2.4 eV can be extracted from this data by assuming that the reactive cross sections are equal at the two different collision energies. This result is listed

Table 2
Measured $O(^3P_j)$ distributions from the $H+O_2$ reaction at 226 nm

Collision energy (eV)	$j=2$	$j=1$	$j=0$	Ref.
1.6	1.0 (03)	0.49 (3)	0.20 (2)	this work
2.4+1.5	1.0 (03)	0.33 (1)	0.16 (1)	this work
2.4	1	0.31	0.145	this work
2.1	1.0 (03)	0.40 (3)	0.19 (3)	[6]
2.5	1.0 (03)	0.30 (3)	0.13 (3)	[6]
statistical	1	0.60	0.20	

in table 2, which also presents the fine-structure distribution at infinite temperature.

We note that the O atom reaction product has a fine-structure distribution that cools with increasing relative collision energy of the reagents. We also list in table 2 the O atom fine-structure distribution for this reaction found by Matsumi et al. [6] using photolysis of HBr and H_2S at 193 nm. It is gratifying to find that our distribution agrees with theirs.

Graff and Wagner [1] have performed a theoretical treatment of the exothermic reverse reaction $O(^3P_j)+OH(^2\Pi)$. They have explicitly taken into account long-range electrostatic and spin–orbit interactions related to the different fine-structure states and have calculated the corresponding potential surfaces. We note here that the $OH(^3\Pi_\Omega)$ and $O(^3P_j)$ give rise to eighteen doubly degenerate potential energy surfaces within 400 cm^{-1}. The transition probability between various surfaces is governed by nonadiabatic couplings. Graff and Wagner found that at collision energies lower than 100 meV (1000 K) only the $O(^3P_{j=2})+OH(^2\Pi_{\Omega=3/2})$ channel is reactive. Transitions between fine-structure states are not expected below collision energies of 0.8–2.1 eV [2]. From the work of Graff and Wagner it might be expected that the reactions proceed adiabatically. The present experimental results, together with those of Matsumi et al., suggest otherwise; that is, nonadiabatic transitions play an important role in the reaction dynamics for $H+O_2\rightarrow OH+O$. Apparently changes in the fine structure occur in the exit channel, caused by the kinetic energy of the recoiling products. Clearly, more theoretical work is needed to understand the $H+O_2$ reaction. Conversely, the present measurements may serve to guide more sophisticated theoretical treatments.

Acknowledgement

The authors are indebted to R.J. Gordon for helpful discussions and for sending us unpublished results, T. Orlando for discussing his REMPI work, and S. Tsuchiya for useful correspondence. HGR and WJvdZ are grateful to the Deutsche Forschungsgemeinschaft and to the Netherlands Organization for Scientific Research, respectively, for postdoctoral fellowships. MJB gratefully acknowledges a GAANN graduate fellowship from the US Department of Education. This work was supported by the National Science Foundation under Grant Nos. 87-05131 and 89-21198.

References

[1] K. Liu, R.G. MacDonald and A.F. Wagner, Intern. Rev. Phys. Chem. 9 (1990) 187;
M.M. Graff and A.F. Wagner, J. Chem. Phys. 92 (1990) 2423; Chem. Phys. Letters 174 (1990) 287.
[2] C.E. Moore, Atomic energy levels, NSRDS-NBS, Vol. 1 Circular No. 35 (US GPO, Washington, 1971).
[3] J. Miyawaki, T. Tsuchizawa, K. Yamanouchi and S. Tsuchiya, Chem. Phys. Letters 165 (1990) 168.
[4] D.J. Bamford, L.E. Jusinski and W.K. Bischel, Phys. Rev. A 34 (1986) 185.
[5] Y. Matsumi and M. Kawasaki, J. Chem. Phys. 93 (1990) 2481.
[6] Y. Matsumi, N. Shafer, K. Tonokura, M. Kawasaki and H.L. Kim, J. Chem. Phys., submitted for publication.
[7] R.J. Gordon, private communication.
[8] Y.-L. Huang and R.J. Gordon, J. Chem. Phys. 93 (1990) 868.
[9] T. Kinugawa, T. Sato, T. Arikawa, Y. Matsumi and M. Kawasaki, J. Chem. Phys. 93 (1990) 3289.
[10] Y.-L. Huang and R.J. Gordon, J. Chem. Phys. 94 (1991) 640.
[11] C.N. Merrow and B.E. Forch, J. Chem. Phys. 93 (1990) 4791.
[12] M.J. Bronikowski, R. Zhang, D.J. Rakestraw and R.N. Zare, Chem. Phys. Letters 156 (1989) 7.
[13] R. Zhang, W.J. van der Zande, M.J. Bronikowski and R.N. Zare, J. Chem. Phys. 94 (1991) 2704.
[14] R.P. Saxon and J. Eichler, Phys. Rev. A 34 (1986) 199.
[15] K.-D. Rinnen, D.A.V. Kliner and R.N. Zare, J. Chem. Phys. 91 (1989) 7514.
[16] G. Sultan, G. Baravian and J. Jolly, Chem. Phys. Letters 175 (1990) 37.
[17] P.G. Carrick and P.C. Engelking, Chem. Phys. Letters 108 (1984) 505.
[18] T.M. Orlando, A.R. Burns, E.B. Steckel and D.R. Jennison, J. Vacuum Sci. Tech. A, in press.
[19] H. Zacharias, K. Meier and K.B. Welge, in: Energy storage and redistribution in molecules, ed. J. Hinze (Plenum Press, New York, 1983).
[20] D.L. Baulch, D.D. Drysdale and D.G. Horne, in: 14th Symposium (International) on Combustion (The Combustion Institute, Pittsburgh, 1973) p. 107.
[21] G.L. Schott, Combustion Flame 21 (1973) 357.
[22] C.T. Bowman, in: 15th Symposium (International) on Combustion (The Combustion Institute, Pittsburgh, 1975) p. 869.
[23] P. Franck and Th. Just, Ber. Bunsenges. Physik. Chem. 89 (1985) 181.

[24] N. Fujii and K.S. Shin, Chem. Phys. Letters 151 (1988) 461.
[25] K. Kleinermanns and J. Wolfrum, J. Chem. Phys. 80 (1984) 1446.
[26] K. Kleinermanns and E. Linnebach, J. Chem. Phys. 82 (1985) 5012.
[27] K. Kleinermanns, E. Linnebach and M. Pohl, J. Chem. Phys. 91 (1989) 2181.
[28] A. Jacobs, H.R. Volpp and J. Wolfrum, Chem. Phys. Letters 177 (1991) 200.
[29] C.F. Melius and R.J. Blint, Chem. Phys. Letters 64 (1979) 183.
[30] S.P. Walch, C.M. Rohlfing, C.F. Melius and C.W. Bauschlicher Jr., J. Chem. Phys. 88 (1988) 6273.
[31] K. Kleinermanns and R. Schinke, J. Chem. Phys. 80 (1984) 1440.
[32] R.C. Weast and M.J. Astle, eds., CRC Handbook of chemistry and physics, 62nd Ed. (CRC Press, Boca Raton, 1981).